

PAPER

## Schottky contact on ultra-thin silicon nanomembranes under light illumination

To cite this article: Enming Song *et al* 2014 *Nanotechnology* **25** 485201

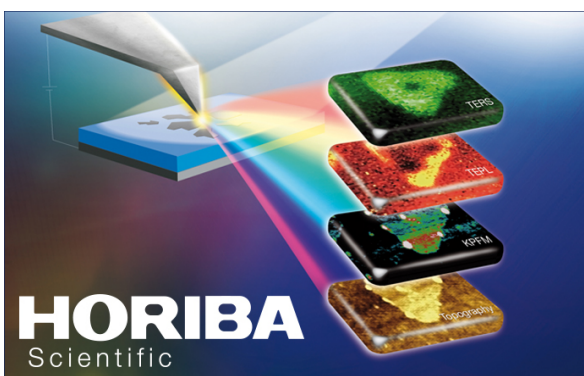
View the [article online](#) for updates and enhancements.

### Related content

- [Ultrahigh sensitivity and gain white light photodetector based on GaTe/Sn : CdS nanoflake/nanowire heterostructures](#)  
Weichang Zhou, Yong Zhou, Yuehua Peng *et al*.
- [Integrated freestanding single-crystal silicon nanowires: conductivity and surfacetreatment](#)  
Chung-Hoon Lee, Clark S Ritz, Minghuang Huang *et al*.
- [Locally hydrazine doped WSe<sub>2</sub> p-n junction toward high-performance photodetectors](#)  
Mengxing Sun, Dan Xie, Yilin Sun *et al*.

### Recent citations

- [Assembly and Self-Assembly of Nanomembrane Materials-From 2D to 3D](#)  
Gaoshan Huang and Yongfeng Mei
- [Nanogranular SiO<sub>2</sub> proton gated silicon layer transistor mimicking biological synapses](#)  
M. J. Liu *et al*



## LIVE WEBINAR

NanoRaman: Correlated Tip-Enhanced Optical Spectroscopy and Scanning Probe Microscopy

Thursday 8 March 15.00 GMT

REGISTER NOW!

[physicsworld.com](http://physicsworld.com)

# Schottky contact on ultra-thin silicon nanomembranes under light illumination

Enming Song<sup>1</sup>, Wenping Si<sup>2</sup>, Ronggen Cao<sup>1</sup>, Ping Feng<sup>3</sup>, Ingolf Mönch<sup>2</sup>, Gaoshan Huang<sup>1,4</sup>, Zengfeng Di<sup>5</sup>, Oliver G Schmidt<sup>2</sup> and Yongfeng Mei<sup>1</sup>

<sup>1</sup>Department of Materials Science, Fudan University, Shanghai 200433, People's Republic of China

<sup>2</sup>Institute for Integrative Nanosciences, IFW Dresden, Helmholtzstr. 20, D-01069, Dresden, Germany

<sup>3</sup>School of Electronic Science & Engineering, Nanjing University, Nanjing 210093, People's Republic of China

<sup>4</sup>National Key Laboratory of Fundamental Science of Micro/Nano-Devices and System Technology, Chongqing University, Chongqing 400030, People's Republic of China

<sup>5</sup>State Key Laboratory of Functional Materials for Informatics, Shanghai Institute of Microsystem and Information Technology, Chinese Academy of Sciences, Shanghai 200050, People's Republic of China

E-mail: [gshuang@fudan.edu.cn](mailto:gshuang@fudan.edu.cn) and [yongfeng.mei@gmail.com](mailto:yongfeng.mei@gmail.com)

Received 20 July 2014, revised 17 September 2014

Accepted for publication 23 September 2014

Published 7 November 2014

## Abstract

By repeating oxidation and subsequent wet chemical etching, we produced ultra-thin silicon nanomembranes down to 10 nm based on silicon-on-insulator structures in a controllable way. The electrical property of such silicon nanomembranes is highly influenced by their contacts with metal electrodes, in which Schottky barriers (SBs) can be tuned by light illumination due to the surface doping. Thermionic emission theory of carriers is applied to estimate the SB at the interface between metal electrodes and Si nanomembranes. Our work reveals that the Schottky contacts with Si nanomembranes can be influenced by external stimuli (like light luminescence or surface state) more heavily compared to those in the thicker ones, which implies that such ultra-thin-film devices could be of potential use in optical detectors.

Keywords: Si nanomembrane, ultra-thin nanomembrane, SOI, Schottky barriers, surface doping

(Some figures may appear in colour only in the online journal)

## 1. Introduction

Inorganic nanomembranes (INMs) with various geometries [1, 2] have shown great promise for potential applications in e.g. flexible electronics [3], metamaterials [4], and strained silicon technology [5]. Schottky barriers (SBs) of metal electrodes on inorganic nanomembranes are often observed to be greatly influenced by surface states [6, 7] and thus play a significant role in devices' electrical properties [8]. Meanwhile, it has been reported that surface doping could dominate the carrier transport in SiNMs when their thickness decreased down to several nanometers [9]. Moreover, the SB difference on double-electrode devices based on SiNMs can offer possibilities to create novel optoelectronic components like photovoltaic cells [8] and persistent photoconductive devices [10]. On the other hand, the contact properties of silicon nanowires and carbon nanotubes have been explored to

clarify the effect of local-illumination by using scanning photocurrent spectroscopy [11]. In addition, a related theory has been reported for energy band alignments of SB at contacts between metal and semiconductor nanostructures [12, 13]. It is worth noting that the electrical properties of ultra-thin SiNMs (~10 nm) under illumination have not been systematically studied, yet, and therefore a detailed investigation of their contacts with metal electrodes [12] is highly demanded.

In this work, we use oxidation and subsequent HF etching [14] to fabricate ultra-thin SiNMs down to 10 nm under a controllable process. By applying local-illumination, the electrical properties of such SiNMs are addressed to understand the charge injection phenomena. We use thermionic emission (TE) theory of carriers to calculate SB heights and explain the origin of carrier transport near SB and illumination tuning effects in the experiments. Besides, we

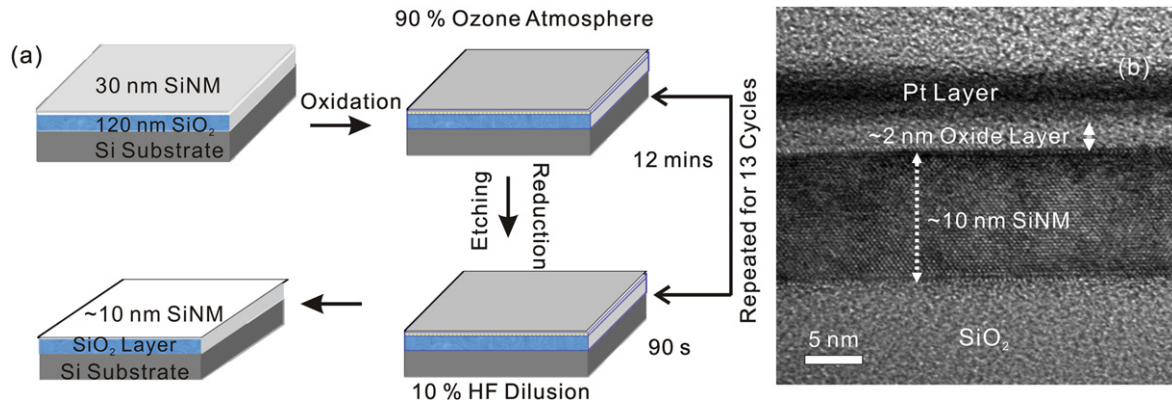


**Figure 1.** (a) The thinning of SiNMs includes two main processes: oxidation and etching. The original 27 nm SiNM was put in 90% ozone atmosphere at RT for 12 min. The top silicon layer was oxidized to SiO<sub>2</sub>. Then the sample was etched by 10% HF solution for 90 s to remove the formed SiO<sub>2</sub>. We repeated the process for 13 cycles. (b) TEM image of a typical ultra-thin SiNM with a thickness of ~10 nm.

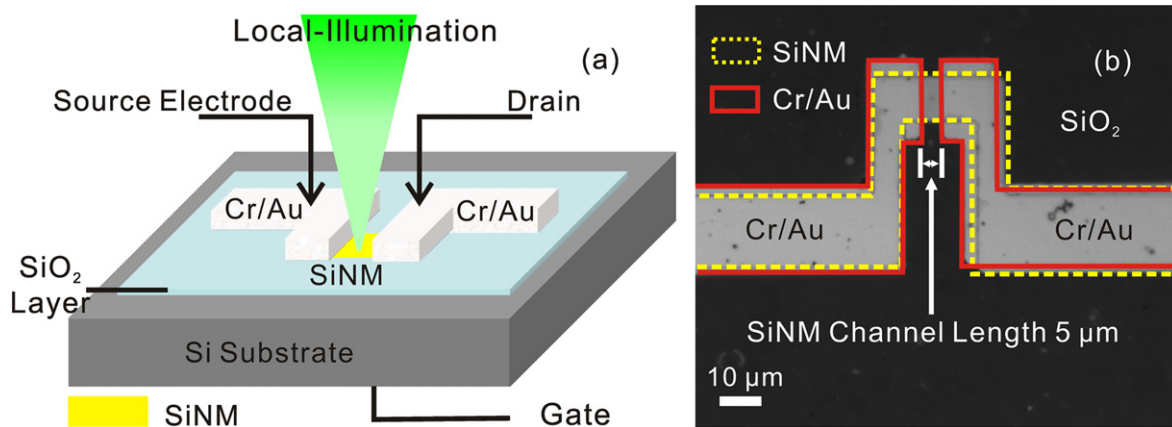


**Figure 2.** (a) Diagram of the SiNM FET device investigated. The test transistor is fabricated based on the 10 nm thickness SiNM. The electrodes are Cr/Au (5/50 nm). (b) Optical microscope image of SiNM FET. Note that the channel is 5 μm long and 18 μm wide.

build up a model for thermo- and photo-induced currents to describe the principle of charge injection.

## 2. Fabrication of ultra-thin SiNMs

The starting material used here is a (0 0 1) bonded silicon-on-insulator (SOI) wafer with a top SiNM thickness of 27 nm, and the SiNM has a boron doping level of  $10^{15} \text{ cm}^{-3}$  which has a resistivity of about  $10 \Omega \text{ cm}$ . The original SiNM was patterned by normal photolithography and then thinned by repeated oxidation and HF etching [14]. This method is used for integrated circuit processing at low temperature. The original SiNM was put in 90% ozone atmosphere at room temperature (RT) for 12 min to oxidize the top Si layer. Then, the sample was etched by 10% HF solution for 90 s, which can thoroughly remove the SiO<sub>2</sub> just formed. We repeated these steps for 13 cycles (see figure 1(a)) to reduce the thickness of SiNM from 27 nm to around 10 nm. The fabrication method is stable and controllable with an average top layer removal rate of 1.31 nm Si per cycle. The final thickness of ultra-thin SiNMs was characterized by a transmission electron microscope (TEM, Philips CM200FEG) and a

typical image is shown in figure 1(b). The Si/SiO<sub>2</sub> interface, a top native oxide layer (~2 nm) and a protecting Pt patterned layer are also shown. The thickness of a SiNM is successfully reduced to ~10 nm, which ensures the preparation of ultra-thin SiNMs.

## 3. Device of SiNM field effect transistors (FETs)

To evaluate the electrical properties of the ultra-thin SiNM, we prepared a FET device based on the thinned SiNM (which is called SiNM FET). The diagram of the final device is shown in figure 2(a), where the Si substrate serves as the back gate. After the thickness reduction, SiNMs were patterned by photolithography. The two-terminal electrodes were prepared by photolithography. The two-terminal electrodes were prepared by depositing Cr/Au (5/50 nm) by e-beam evaporation, combined with a photoresist-liftoff. Subsequently, the interfaces at Cr/Si contacts are strengthened by rapid thermal annealing at 500 °C for 3 min in ambient Ar gas with a ramping rate of  $16 \text{ °C s}^{-1}$ . Figure 2(b) shows the optical microscope image of the transistor fabricated on a 10 nm SiNM, whose channel is 5 μm long and 18 μm wide. The local illumination of the channel is accomplished by a 633 nm

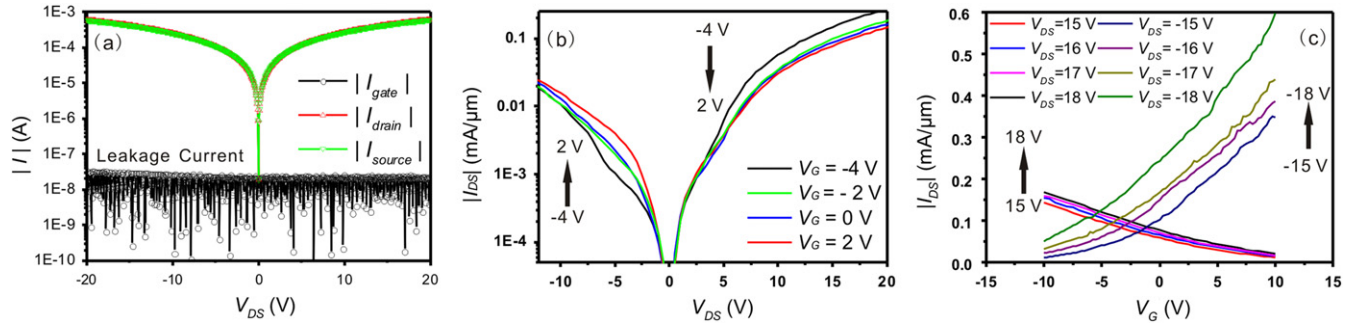


**Figure 3.** (a) The currents at gate, drain and source electrodes. The SiNM is exposed to light at RT. The drain voltage is changed from  $-20$  to  $20$  V and the gate voltage is fixed at  $0$  V. (b) Typical  $I_{DS}$ – $V_{DS}$  curves of SiNM FET in the dark. Along the direction of the black arrows,  $V_G$  increases from  $-4$  V to  $2$  V. (c) Transfer characteristics of SiNM FET. Along the direction of the arrows, the bias voltage  $V_{DS}$  changes by steps of  $1$  V.

laser with a maximum power density of  $25 \mu\text{W} \mu\text{m}^{-2}$  on the sample surface tested by a SCIENTECH 312 Power and Energy Meter and the focal spot has a diameter of  $5 \mu\text{m}$ . The device temperature is controlled by a hotplate and real-time temperature is tested by a FLUKE 51 thermometer. The electrical characteristic of the SiNM FET was measured by a semiconductor parameter analyzer (Keithley, SCS-4200).

#### 4. Basic electrical property of SiNM FETs

We investigate charge-transport mechanisms of ultra-thin SiNM by injecting charges. In principle, there are three types of charge injection at the interface between metal and semiconductor: thermal emission, tunneling, and electron–hole recombination in the depletion region. Noting that the SiNM channel has a length of  $\sim 5 \mu\text{m}$  and a thickness of around  $10$  nm, it is expected that the voltage bias has a minor effect on the SB at the contacts [8].

Figure 3(a) shows the currents at gate, drain and source electrodes in the illuminated device, as displayed by  $|I_{\text{gate}}|$ ,  $|I_{\text{drain}}|$  and  $|I_{\text{source}}|$ , respectively. The leakage current through the gate is almost five orders of magnitude lower than  $|I_{\text{drain}}|$  and  $|I_{\text{source}}|$  after  $V_{DS}$  reaches the threshold voltage. The low leakage current in SiNM [15] assures leakage current can be neglected in the following discussion. Figure 3(b) exhibits how the gate voltage  $V_G$  modulates the current, where  $V_G$  changes from  $-5$  to  $5$  V under dark condition. The characteristic of the device exhibits ambipolar behavior, which is usually observed in SB type FET [16]. The results shown in figure 3(b) indicate that the drain and source contacts are Schottky type with a stable threshold voltage due to full depletion. We also obtained the  $I_{DS}$ – $V_G$  curves with fixed  $V_{DS}$ , as plotted in figure 3(c). The  $I_{DS}$ – $V_G$  curves at different  $V_{DS}$  indicated that the device has an ambipolar behavior: for negative  $V_{DS}$ , the current increases with increasing  $V_G$ , exhibiting an n-type behavior; for positive  $V_{DS}$ , the current decreases with increasing  $V_G$ , hence exhibiting a p-type behavior, which suggests that the channel is n-type for negative  $V_{DS}$  and p-type for positive  $V_{DS}$ .

#### 5. Carrier transportation under light illumination

Previous experimental work showed that changing the surrounding temperature can be used to tune the SB height [17]. Here, we heated SiNM in the dark at different temperature (inset of figure 4(a)) to exhibit the thermo-effect of SiNM [18]. In addition, we also tried to reveal the influence of light illumination on the electrical performances of the SiNM FET. The currents between the channel in the dark and under light illumination are plotted in figure 4(a). The Schottky type characteristic is obvious in all the curves [19]. It is well known that light illumination is an effective method of charge injection [10], for it brings more carriers, and illumination can also modulate the depletion region and tune the SB height [12]. We can see from figure 4(b) that the  $I_{DS}$  is strongly increased under light illumination. Considering the ideal situation of a stable carrier density, we use TE of hole across SB to model the  $I_{DS}$ – $V_{DS}$  characteristics in figure 4(c). We approximate the voltage drop across the SB as a fraction parameter  $C$  of the reversed voltage applied across the device. From the equation for thermionic-emission current across SB, the relation of the current and applied bias voltage could be written as:

$$I_{DS} = SA^*T^2 \exp\left(-\frac{e\phi_{B0}}{kT}\right) \left\{ \exp\left(\frac{-eCV_{DS}}{kT}\right) - 1 \right\}, \quad (1)$$

where  $T$  is the absolute temperature,  $S$  is the SiNM channel cross-sectional area,  $\phi_{B0}$  is the SB height at zero bias,  $A^*$  is the effective Richardson constant ( $32 \text{ A cm}^{-2} \text{ K}^{-2}$  for p-type Si) [20],  $e$  is the electronic charge,  $k$  is the Boltzmann constant.  $C$  stands for a fraction of the voltage applied across the SB [21]. From equation (2), we can regard the former part of equation (1) as a constant  $I_0$ :

$$I_0 = SA^*T^2 \exp\left(-\frac{e\phi_{B0}}{kT}\right), \quad (2)$$

which can be obtained by from the intercept value [22] of  $\ln I$ – $V$  curve to zero applied bias-voltage in figure 4(b) and the  $\phi_{B0}$  values can be calculated from equation (2) by zero-bias methods [13]. With gate voltage fixed to zero, the  $\phi_{B0}$  to the three solid dots curves in figure 4(c) (referring to dark current

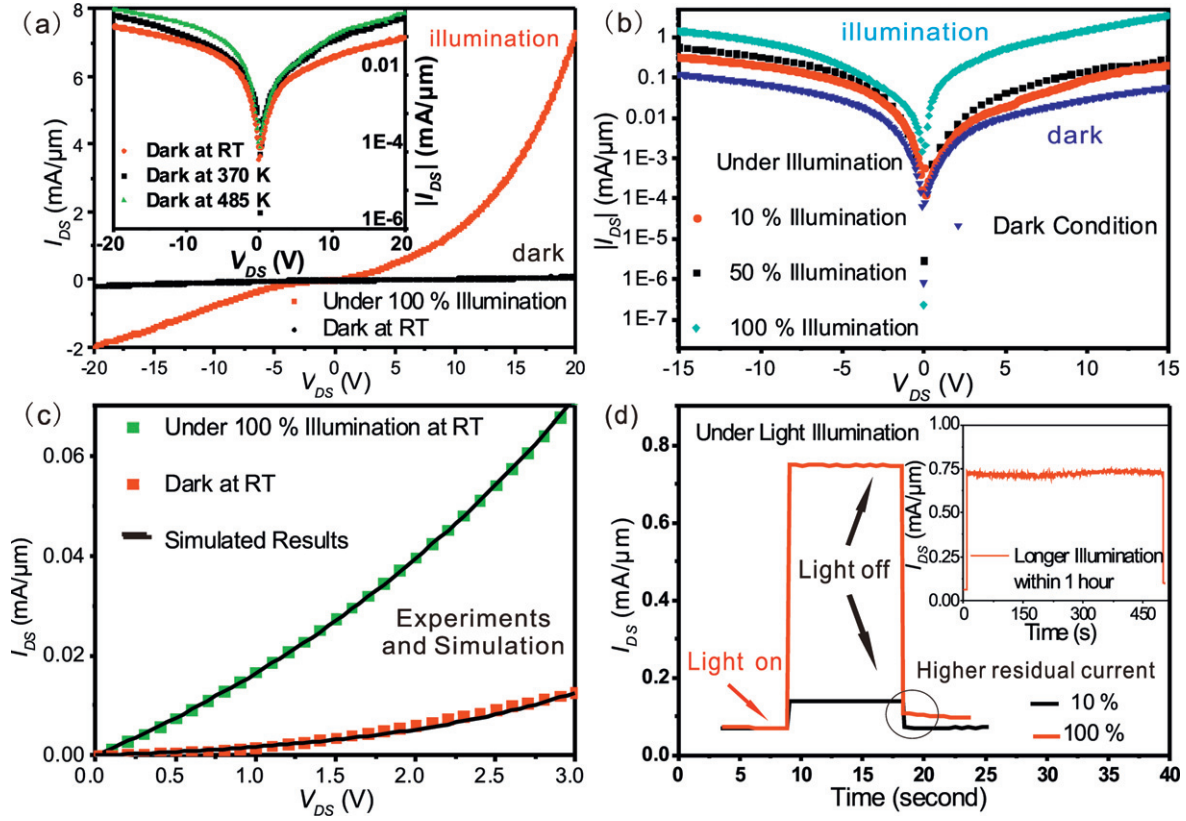


**Figure 4.** (a)  $I_{DS}$ – $V_{DS}$  properties of the SiNM. The dark current and photocurrent are shown. The inset:  $|I_{DS}|$ – $V_{DS}$  curves. The device is put in the dark at 300, 370 and 485 K. (b)  $|I_{DS}|$ – $V_{DS}$  properties of the SiNM in the dark and under illumination at RT.  $V_G=0$  V. We test electrical properties at 300 K in the dark and under different illumination power densities ( $2.5$ ,  $12.5$  and  $25 \mu\text{W } \mu\text{m}^{-2}$ ) from  $-15$  to  $15$  V. (c)  $I_{DS}$ – $V_{DS}$  plots of tested and simulated results from  $0$  to  $3$  V in the dark and under illumination at RT. The simulation is obtained by the TE model. (d) Dynamic electrical characterization of SiNM. The currents of on- and off-states by switching illumination are shown. We turn on the light at  $8$  s and then switch it off at  $18$  s. The illumination power is chosen as  $2.5 \mu\text{W } \mu\text{m}^{-2}$  (10%) and  $25 \mu\text{W } \mu\text{m}^{-2}$  (100%). The circle shows a higher residual current after illumination power (100%) is turned off. The inset displays the photocurrent in continuous light illumination (100%) of  $1$  h.

at RT, photocurrent (50%) and photocurrent (100%) at RT respectively) are  $0.363$  eV,  $0.559$  eV, and  $0.701$  eV, respectively. In figure 4(c), the two black lines are corresponding current values simulated by TE theory and one can see that the calculation fits our experimental results well.

SiNMs can absorb photons from illumination when light penetrates into the nanomembrane [23]. The relation between illumination power  $P$  in the nanomembrane and penetration depth  $x$  can be written as equation (3):

$$P = P_0 \exp(-\alpha x), \quad (3)$$

where  $P_0$  is the power at the surface and  $\alpha$  is the absorption coefficient, which is a property of a material defined as the fraction of light absorbed, related to material property and light wavelength [24–26]. It can be mathematically deduced that for a SiNM with thickness of  $d$  the light absorbance per unit thickness  $\left(\frac{P_0 - P_0 \exp(-\alpha d)}{d}\right)$  should become large in the case of a small  $d$ . This special characteristic of our ultra-thin membrane makes nanomembranes have great potential applications as sensitive photoelectric detectors.

The illumination effect on the main electrical parameters such as  $\Phi_{B0}$  and  $I_0$  in an n-Si diode has previously been investigated [27]. It showed that the electrical characteristics

of the SB contacts are significantly affected by illumination. However, the illumination on SiNM produced both photo-generated carriers and heating effects. It can be supposed that the nanomembrane absorbs different energy from different wavelength light, which is subsequently converted to dissimilar amount of heat [28]. To investigate this in more details, we measured  $I_{DS}$  under illumination with different power density, the results are shown in figure 4(d), where both light ‘on’ and ‘off’ states are depicted. We can estimate the current in the ‘on’ state by using equation (4) [29]:

$$I_{on} = I_{dark}(T) + I_{PC} \approx I_{dark}(T) + k\psi, \quad (4)$$

where  $I_{on}$  is the current under illumination and  $I_{dark}(T)$  corresponds to the thermally activated current in the dark.  $I_{PC}$  is the photo current and is a function of illumination intensity [30]. Here, the photocurrent can be expressed as  $k\psi$ , where  $\psi$  is the photon flux and  $k$  is a constant [29]. Therefore, the current under illumination consists of two parts: (1) TE and (2) photocurrent.

When the illumination is turned on, the current increases because both thermo current and photocurrent contribute to the current (see equation (4)). On the other hand, when the illumination is off,  $I_{PC}$  will disappear immediately but the

temperature of the SiNM will decrease during the cooling relaxation time, thus  $I_{\text{dark}}(T)$  will stay at a higher value compared to that at RT. This phenomenon can be observed in figure 4(d) where  $I_{\text{dark}}$  (red line) remains at a higher level (the circle in figure 4(d)) after the illumination is switched off. The inset shows the continuous laser illumination of 1 h leads to a stable photocurrent, and the value of the photocurrent is same to that under short time illumination. In our experiment, we found that the dark current at 485 K fits well with the current after the illumination of  $25 \mu\text{W} \mu\text{m}^{-2}$  is turned off. Therefore, we can make a rough estimation that the stable temperature of the SiNM under  $25 \mu\text{W} \mu\text{m}^{-2}$  laser illumination is around 485 K.

## 6. Contact properties of ultra-thin SiNMs based on band edge alignment

We investigate the special electrical properties of the metal–semiconductor contacts when the semiconductor thickness decreases down to nanometers. Here, we discuss the alignment of bands and investigate the special characteristic of contacts on ultra-thin SiNM.

It is known that the contact type depends on the positions of the Fermi levels and the band structures of both the metal and the semiconductor [13]. The SB height at metal/semiconductor (MS) contact can be calculated by:

$$\Phi_{\text{B}} = \phi - \chi, \quad (5)$$

where  $\Phi$  is the metal work function and  $\chi$  is the semiconductor electron affinity. However, at the contact interface, Heine [31] first pointed out that the wave functions of the metal electrons tailed into the semiconductor in the energy range and these metal-induced gap states represent the fundamental mechanism that determined the SB height, which is called Fermi level pinning [13], and an electrostatic potential causes the valence and conduction bands to bend near the interface [32]. For nanosemiconductor contacts, there are two different groups. The first group includes nanowires and nanotubes. It has been suggested theoretically that metal-induced gap states have a weaker impact on the band alignment due to electrostatics at reduced cross section [33]. The second group is ultra-thin nanomembranes. Interface gap states and large surface area can have a strong influence on Fermi level pinning on nanomembranes due to their large surface-to-volume ratios.

Generally, the realignment of band levels is determined by three factors: metal Fermi level, semiconductor Fermi level, and gap states. In ultra-thin SiNM, a large amount of surface dopants owing to the huge contact area can also modulate the SB [8]. In bulk, heavily doping the semiconductor near the contact can overcome the SB by reducing the depletion width, which allows carriers to tunnel through the barrier. However, establishing the proper band bending in nanotubes and small nanowires is difficult and requires much more doping as the cross section area decreases [13]. In contrast, the ultra-thin nanomembrane is far more sensitive to doping at the surface, which is called surface doping. The

special characteristic of the contact on the SiNM is supposed to be influenced easily by surface doping and is able to make lower contact resistivity by proper dopant density, which is increasingly difficult in bulk material, nanotubes or nanowires. Such surface doping is sensitive to external stimuli for instance light illumination [12].

On the other hand, large contact or cross section area causes carriers injection in nanomembranes much more easily under illumination. Meanwhile the essential effect of illumination on MS contacts reveals that the light also can tune the shape of the SB. More specifically, the depletion width, which depends exponentially on the doping density, changes with persistent light illumination [12]. For bulk materials, the depletion width is relatively small compared to nanoscale materials, where depletion widths can be up to several hundred nanometers wide [34, 35]. It means that when illumination on, depletion width at nanoscale MS interfaces (including nanomembranes and nanowires) is reduced more sensitively than bulk material, as displayed as blue dotted line in figure 5(a). Thus, the current significantly increased in figure 4(a). The full depletion of the SiNM makes  $I_{\text{DS}}-V_{\text{DS}}$  characteristics determined by two side contacts, and the carrier transport is to some extent totally determined by built-in potential between two contacts, resulting in a stable threshold voltage in figure 3(b). This is an ideal situation to avoid short cut and kink effects [36].

Before we discuss the carrier transport mechanism inside the SiNM, it is highly necessary to take account into the SB height inhomogeneities in our device. Noting that our SiNM has  $5 \mu\text{m}$  long channel (500 times longer than thickness), it should be considered that thickness fluctuations and strains inside SiNM are different at drain or source contacts. The metal's electron wave function decays into silicon [37] and is believed to be sensitive to Si surface status at both contacts, which causes different band bending [10]. Under illumination, electron–hole pairs are effectively generated in the SiNM. With the increase of non-equilibrium carrier concentration, the electron's and hole's quasi Fermi levels are modulated, and surface recombination is enhanced [13], as depicted in figure 5(a). The photo-generated electrons are swept towards the barrier at the interface due to the influence of the electric field applied, whereas holes are accelerated towards the metal [8]. Even at low bias,  $I_{\text{DS}}$  in illuminated SiNM is increased remarkably.

We discuss this in more detail. The fluctuation of  $V_{\text{DS}}$  has a big influence on the density of free electrons in the channel from metal electrodes. When positive voltages ( $V_{\text{DS}} > 0$ ) are applied to the drain contact, as illustrated in figure 5(b), the band edge bends downward at the drain side. At low voltages, the barrier  $\Phi_{\text{h}}$  is too high for hole injection, and the current is low. With increasing voltage,  $\Phi_{\text{h}}$  is no longer a sharp barrier for holes and respective injection becomes much easier. After one threshold voltage is achieved, the current increases exponentially. In contrast, the injection of electrons at the source contact is difficult due to the barrier  $\Phi_{\text{e}}$  [21]. Similar assumptions hold for negative voltages ( $V_{\text{DS}} < 0$ ) as shown in figure 5(c).

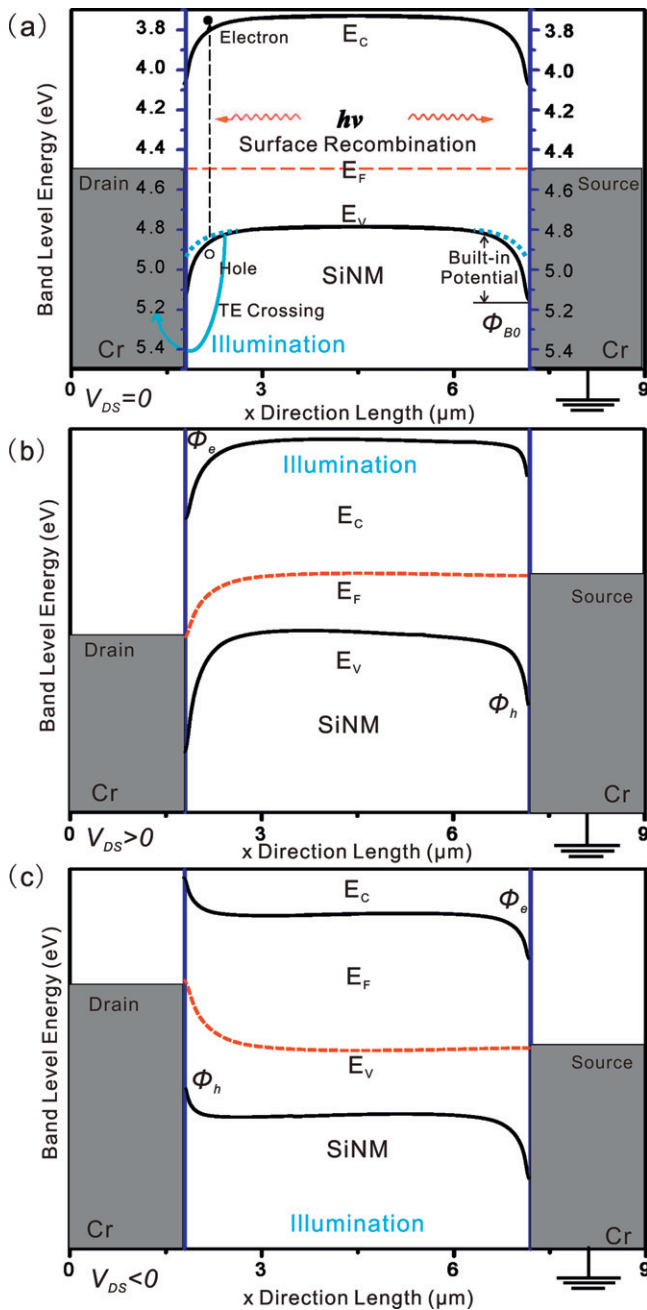


**Figure 5.** Ideal band edge alignments of the device for (a) SiNM in the dark and under illumination when  $V_{DS}=0$  V. The SiNM absorbs light and electron–hole pairs are generated. The illumination increases the effective SB height and changes the surfaces. (b)  $V_{DS}>0$  and (c)  $V_{DS}<0$  V of SiNM under illumination.  $E_F$  is the Fermi level,  $E_C$  is the bottom of the conduction band and  $E_V$  is the top of the valence band.  $\Phi_e$  is the electron injection barrier and  $\Phi_h$  is the barrier for holes.

Here we just consider the ideal situation of band alignments in absence of the Fermi level pinning. The resistivity of SiNM suggests an acceptor doping level  $N_A$  of about  $10^{15} \text{ cm}^{-3}$  [38]. At 300 K, the valence band effective state concentration  $N_V$  of Si is approximately  $10^{10} \text{ cm}^{-3}$  [39]. In this non-degenerate case, the difference between semiconductor Fermi level  $E_F$  and valence band  $E_V$  can be estimated by  $E_F - E_V = -k_B T \times \ln(N_V/N_A) \approx 0.3 \text{ eV}$  in figure 5(a),

where  $k_B$  is the Boltzmann constant and  $T$  the temperature. According to the fact that the electron affinity of Si is 4.05 eV with a 1.12 eV band gap and the Cr work function is around 4.5 eV, the theoretical SiNM to Cr SB height is calculated as  $\Phi_{B0} = (4.05 + 1.12 - 0.3) - 4.5 = 0.37 \text{ eV}$ , which agrees with the experimental measured value of 0.363 eV. The carriers at low illumination are able to surmount the lower barriers and therefore current transport will be dominated by surface recombination and current flowing through the patches of lower SB height. As the illumination intensity is increased, the behavior of surface recombination is strengthened and meanwhile more carriers (i.e. holes) have sufficient energy to surmount the higher barrier [40] in figure 5(a). Therefore, the SB height of the p-type FET for holes  $\Phi_h$  is calculated to be 0.701 eV. This result indicates that the illumination effect on the electrical properties of SiNMs is significant and these devices can be used as an optical sensor for optoelectronic applications [10].

## 7. Conclusion

In summary, we have investigated the tuning effect of local-illumination to the SB contact on ultra-thin SiNM. These nanomembranes are more sensitive to surface doping densities than bulk material due to a large surface-to-volume ratio. Illumination and higher temperature increase the non-equilibrium carrier concentration and influence the surface doping density. We also put forth a model to explain the charge injection and the observed increase in both thermo- and photo-currents. There is great potential for semiconductor ultra-thin membranes to be applied into optoelectronic application as a novel type of membrane device.

## Acknowledgments

This work was supported by the National Natural Science Foundation of China (Nos. 51322201 and 51102049); ‘Shu Guang’ project by Shanghai Municipal Education Commission and Shanghai Education Development Foundation; Specialized Research Fund for the Doctoral Program of Higher Education (No. 20120071110025); Science and Technology Commission of Shanghai Municipality (Nos. 12520706300 and 14JC1400200), and Visiting Scholar Foundation of National Key Laboratory of Fundamental Science of Micro/Nano-Devices and System Technology in Chongqing University (No. 2014MS03). Part of the experimental work has been carried out in Fudan Nanofabrication Laboratory.

## References

- [1] Rogers J A, Lagally M G and Nuzzo R G 2011 Synthesis, assembly and applications of semiconductor nanomembranes *Nature* **477** 46

- [2] Cho A 2006 Pretty as you please, curling films turn themselves into nanodevices *Science* **313** 164
- [3] Sun Y and Rogers J A 2007 Inorganic semiconductors for flexible electronics *Adv. Mater.* **19** 1897
- [4] Smith E J, Liu Z, Mei Y F and Schmidt O G 2010 Combined surface plasmon and classical waveguiding through metamaterial fiber design *Nano Lett.* **10** 1
- [5] Roberts M M, Klein L J, Savage D E, Slinker K A, Friesen M, Celler G, Eriksson M A and Lagally M G 2006 Elastically relaxed free-standing strained-silicon nanomembranes *Nat. Mater.* **5** 388
- [6] Heinze S, Tersoff J, Martel R, Derycke V, Appenzeller J and Avouris P 2002 Carbon nanotubes as Schottky barrier transistors *Phys. Rev. Lett.* **89** 106801
- [7] Freitag M, Radosavljevic M, Zhou Y, Johnson A T and Smith W F 2001 Controlled creation of a carbon nanotube diode by a scanned gate *Appl. Phys. Lett.* **79** 3326
- [8] Feng P, Mönch I, Harazim S, Huang G S, Mei Y F and Schmidt O G 2009 Giant persistent photoconductivity in rough silicon nanomembranes *Nano Lett.* **9** 3453
- [9] Zhang P, Tevaarwerk E, Park B N, Savage D E, Celler G K, Knezevic I, Evans P G, Eriksson M A and Lagally M G 2006 Electronic transport in nanometre-scale silicon-on-insulator membranes *Nature* **439** 703
- [10] Feng P, Mönch I, Huang G S, Harazim S, Smith E J, Mei Y F and Schmidt O G 2010 Local-illuminated ultrathin silicon nanomembranes with photovoltaic effect and negative transconductance *Adv. Mater.* **22** 3667
- [11] Gabor N M, Zhong Z, Bosnick K, Park J and McEuen P L 2009 Extremely efficient multiple electron-hole pair generation in carbon nanotube photodiodes *Science* **325** 1367
- [12] Kamieniecki E 2012 Defect specific photoconductance: carrier recombination through surface and other extended crystal imperfections *J. Appl. Phys.* **112** 063715
- [13] Léonard F and Talin A A 2011 Electrical contacts to one- and two-dimensional nanomaterials *Nat. Nanotechnology* **6** 773
- [14] Scott S A and Lagally M G 2007 Elastically strain-sharing nanomembranes: flexible and transferable strained silicon and silicon-germanium alloys *J. Phys. D: Appl. Phys.* **40** R75
- [15] Michalas L, Exarchos M, Papaioannou G J, Kouvatso D N and Voutsas A T 2007 An experimental study of the thermally activated processes in polycrystalline silicon thin film transistors *Microelectron. Reliab.* **47** 2058
- [16] Hasegawa T, Mattenberger K, Takeya J and Batlogg B 2004 Ambipolar field-effect carrier injections in organic Mott insulators *Phys. Rev. B* **69** 245115
- [17] Soyul M, Al-Ghamdi A A and Yakuphanoglu F 2012 Influence of illumination intensity and temperature on the electrical characteristics of an Al/p-GaAs/In structure prepared by thermal evaporation *Microelectron. Eng.* **99** 50
- [18] Wenjun L, Keivan E-Y, Rozana H and Mehdi A 2006 Modeling and data for thermal conductivity of ultrathin single-crystal SOI layers at high temperature *IEEE Trans. Electron Devices* **53** 1868
- [19] Léonard F and Talin A A 2006 Size-dependent effects on electrical contacts to nanotubes and nanowires *Phys. Rev. Lett.* **97** 026804
- [20] Cherif A, Jomni S, Hannachi R and Beji L 2013 Electrical investigation of the Al/porousSi/p<sup>+</sup>-Si heterojunction *Physica B* **409** 10
- [21] Zaremba-Tymieniecki M and Durrani Z A K 2011 Schottky-barrier lowering in silicon nanowire field-effect transistors prepared by metal-assisted chemical etching *Appl. Phys. Lett.* **98** 102113
- [22] Faraga A A M, Asheryb A, Ahmed E M A and Salem M A 2010 Effect of temperature, illumination and frequency on the electrical characteristics of Cu/p-Si Schottky diode prepared by liquid phase epitaxy *J. Alloys Compd* **495** 116
- [23] Khan S A, Al-Agel F A, Faidah A S, Yagmour S J and Al-Ghamdi A A 2010 Characterization of Se<sub>88</sub>Te<sub>12</sub> nanostructured chalcogenide prepared by ball milling *Mater. Lett.* **64** 1391
- [24] Al-Ghamdi A A, Khan S A, Nagat A and Abd El-Sadek M S 2010 Synthesis and optical characterization of nanocrystalline CdTe thin films *Opt. Laser Technol.* **42** 1181
- [25] Khan Z H, Khan S A, Salah N, Habib S, Abdallah S M and Al-Ghamdi A A 2010 Effect of composition on electrical and optical properties of thin films of amorphous Ga<sub>x</sub>Se<sub>100-x</sub> nanorods *Nanoscale Res. Lett.* **5** 1512
- [26] Khan S A, Al-Agel F A and Al-Ghamdi A A 2010 Optical characterization of nanocrystalline Se<sub>85</sub>Te<sub>10</sub>Pb<sub>5</sub> and Se<sub>80</sub>Te<sub>10</sub>Pb<sub>10</sub> chalcogenides *Superlattice Microstruct.* **47** 695
- [27] Uslu H, Dökme İ, Afandiyeva I M and Altundal Ş 2010 Illumination effect on I-V, C-V and G/w-V characteristics of Al-TiW-Pd<sub>2</sub>Si/n-Si structures at room temperature *Surf. Interface Anal.* **42** 807
- [28] Liu X, Wu X M and Ren T L 2011 In situ and noncontact measurement of silicon membrane thermal conductivity *Appl. Phys. Lett.* **98** 174104
- [29] Michalas L, Syntychaki A, Koutsourelis M, Papaioannou G J and Voutsas A T 2012 A temperature study of photosensitivity in SLS polycrystalline silicon TFTs *Microelectron. Reliab.* **52** 2508
- [30] Chaudhary N, Bahishti A A and Zulfeqar M 2012 Photoconductivity of Se<sub>85-x</sub>Te<sub>15</sub>Hg<sub>x</sub> thin films *Physica B* **407** 2267
- [31] Heine V 1965 Theory of surface states *Phys. Rev.* **138** A1689
- [32] Mönch W 1999 Barrier heights of real Schottky contacts explained by metal-induced gap states and lateral inhomogeneities *J. Vac. Sci. Technol. B* **17** 1867
- [33] Chen Z H, Appenzeller J, Knoch J, Lin Y M and Avouris P 2005 The role of metal-nanotube contact in the performance of carbon nanotube field-effect transistors *Nano Lett.* **5** 7
- [34] Mueller T, Xia F, Freitag M and Tsang J 2009 Role of contacts in graphene transistors: a scanning photocurrent study *Phys. Rev. B* **79** 245430
- [35] Gammon P M et al 2013 Modeling the inhomogeneous SiC Schottky interface *J. Appl. Phys.* **114** 223704
- [36] Francis P et al 1995 Moderate inversion model of ultrathin double-gate nMOS/SOI transistors *Solid-State Electron.* **38** 171
- [37] Mönch W 1990 On the physics of metal-semiconductor interfaces *Rep. Prog. Phys.* **53** 221
- [38] Beadle W F, Tsai J C and Plummer C D 1985 *Quick Reference Manual for Semiconductor Engineers* (New York: Wiley)
- [39] Shur M, Simin G, Rumyantsev S, Jain R and Gaska R 2010 *Fundamentals of III-V Semiconductor MOSFETs* (Berlin: Springer) p 379
- [40] Sullivan J P, Tung R T, Pinto M R and Graham W R 1991 Electron transport of inhomogeneous Schottky barriers: a numerical study *J. Appl. Phys.* **70** 7403